Electron Cyclotron Heating Modification of Alfvén Eigenmode Activity in DIII-D

M.A. Van Zeeland[1], W.W. Heidbrink[2], S.E. Sharapov[3], D. Spong[4], A. Cappa[5], X. Chen[1], C. Collins[1], M. García-Muñoz[6], N.N. Gorelenkov[7], G.J. Kramer[7], P. Lauber[6], Z. Lin[2] and C. Petty[1]

[1]General Atomics, P.O. Box 85608 San Diego, California 92186-5608, USA
[2]University of California at Irvine, Irvine, CA 92697, USA
[3]CCFE, Culham Science Centre, Abingdon, Oxon, OX14 3DB, UK
[4]Oak Ridge National Laboratory, Oak Ridge, TN 37830, USA
[5]Laboratorio Nacional de Fusion -CIEMAT. 28040 Madrid, Spain
[6]Max-Planck-Institut fur Plasmaphysik, Euratom Association, Garching, Germany.
[7]Princeton Plasma Physics Laboratory, PO Box 451, Princeton, NJ 08543-0451, USA

Corresponding Author: vanzeeland@fusion.gat.com

Abstract:

Recent experiments have identified the primary factors causing a large variation in neutral beam driven reversed shear Alfvén eigenmode (RSAE) activity brought about by localized electron cyclotron heating (ECH) in DIII-D plasmas. It is found that during intervals when the geodesic acoustic mode (GAM) frequency at q_{min} is elevated and the calculated RSAE minimum frequency, including contributions from thermal plasma gradients, is very near or above the nominal TAE frequency (f_{TAE}), RSAE activity is not observed or RSAEs with a much reduced frequency sweep range are found. This condition is primarily brought about by ECH modification of the local electron temperature (T_e) which can raise both the local T_e at q_{min} as well as its gradient. A q-evolution model that incorporates this reduction in RSAE frequency sweep range is in agreement with the observed spectra and appears to capture the relative balance of TAE or RSAE-like modes throughout the current ramp phase of over 38 DIII-D discharges. Detailed ideal MHD calculations using the NOVA code hav been carried out for the ECH injection near q_{min} case, where no frequency sweeping RSAEs are observed, and the analysis shows the typical RSAE is no longer an eigenmode of the system. The remaining mode is strongly coupled to TAEs and has no frequency variation with q_{min}.

1 Introduction

Localized electron cyclotron heating (ECH) can have a dramatic effect on neutral beam driven Alfvén eigenmode (AE) activity as was first demonstrated in DIII-D reversed magnetic shear plasmas [1, 2, 3] and later on several other devices worldwide including Heliotron-J [4] and TJ-II [5]. The most commonly observed effect on DIII-D is a

shift in the dominant observed modes from a mix of reversed shear Alfvén eigenmodes (RSAEs) [6] and toroidicity induced Alfvén eigenmodes [7] (TAEs) to a spectrum of weaker TAEs when ECH is deposited near the shear reversal point (q_{min}) [1, 2]. ECH deposition near the magnetic axis typically increases the unstable mode amplitudes and resultant fast ion transport. Due to the fact that localized electron heating can impact essentially all aspects of AEs, including mode drive, damping, and the ideal eigenmode itself, a satisfactory explanation for this effect in DIII-D has been elusive. Mode stability is altered through modification of the different damping channels (electron collisional and electron Landau in particular, and even continuum damping through pressure or rotation induced changes to the modes and continuum), mode drive (T_e directly impacts electron drag on fast ions), and the AEs themselves through coupling to sound waves via changes to T_e/T_i [8].

A recent DIII-D experiment to understand the physical mechanisms responsible for the observed shift in RSAE activity with ECH utilized a simplified oval geometry and, in addition to ECH injection location, included variations of current ramp rate, ECH injection timing, beam injection geometry (on/off-axis), and neutral beam power. Essentially all variations carried out in this experiment were observed to change the impact of ECH on AE activity significantly. It is shown that the ratio of the predicted RSAE minimum frequency (Eqn. 3) to the TAE frequency is the dominant factor determining the presence of typical frequency sweeping RSAEs [3], similar to the so-called beta suppression mechanism put forward to explain the absence of typical frequency sweeping RSAEs in spherical tokamaks [9]. In the last section (Section 4), analysis from the ideal MHD code NOVA [10], of an ECH case with no observed RSAE activity, shows that the typical frequency sweeping RSAE is no longer an eigenmode of the system.

2 Discharge Background and Reproduction of Historical ECH/AE Results in Oval Plasmas

The majority of discharges presented in this paper utilize an oval (elongation, $\kappa \approx 1.5$) shaped L-mode deuterium plasma with either no ECH or radial launch, 2nd harmonic, 110 GHz ECH directed to two possible locations, one near the magnetic axis and the other near mid-radius (chosen to be near q_{min} during the current ramp portion of the discharge). In these $B_T = 2.05$ T discharges, 75-80 kV sub-Alfvénic neutral beam injection begins at $t = 300$ ms and continues while the plasma current (I_p) is ramping up at a constant rate of 0.8 MA/s until reaching approximately 1.2 MA at $t = 1100$ ms.

Early neutral beam injection during the current ramp phase produces a variety of Alfvénic activity in these DIII-D plasmas including toroidicity induced Alfvén eigenmodes, reversed shear Alfvén eigenmodes, and linearly coupled RSAEs and TAEs [2]. Spectrograms showing the rich variety of modes that are possible as well as the change in mode activity as ECH is directed to the two different steering locations (near the magnetic axis and near q_{min}) are presented in Figure 1. In this figure, as well several others throughout this paper, a composite spectrogram is constructed by averaging the cross power spec-

trum of several adjacent ECE channels. Discharge 157737 in Figure 1a is a reproduction of a very well documented beam driven AE discharge in DIII-D (142111) that has been studied and modeled extensively with great success [13]. It was the intent of this experiment to begin with this well understood discharge and then move away from it using ECH. Discharges 157736 and 157735 have ECH injection beginning at $t = 300$ ms near the magnetic axis and q_{min} respectively. Consistent with historical results carried out in Dee shaped plasmas [1, 2] these new oval discharges show a radical shift in AE activity from a multitude of TAEs and RSAEs with ECH near the magnetic axis to a discharge that is strongly TAE dominated with very little, if any, observed frequency sweeping RSAEs with ECH near q_{min}.

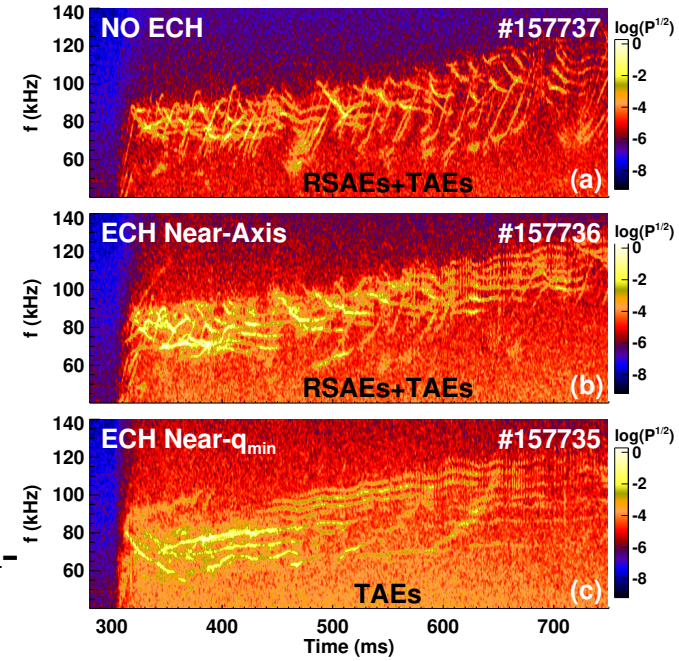

FIG. 1: Combined ECE power spectra for discharges (a) 157737 with NO ECH, (b) 157736 with ≈1.1 MW ECH near the magnetic axis, and (c) 157735 with ≈1.9 MW ECH near q_{min}.

3 Model for RSAE Frequency Evolution and Comparison with Measurements

To aid in the interpretation of these results, a model for the RSAE spectral evolution throughout the current ramp is employed. Similar models have been described in the past and are frequently used to identify the temporal evolution of q_{min} through so-called AE or MHD spectroscopy [12]. The model here is based on constraining the RSAE frequency sweep to be between some minimum frequency ($f_{RSAE-min}$) [11, 14] and the TAE frequency (f_{TAE}). The RSAE minimum frequency lies above that of the geodesic acoustic mode (f_{GAM}) and below the TAE frequency (f_{TAE}). The reduction in RSAE frequency sweep range is a well known effect, the RSAE minimum frequency is shifted above the local GAM frequency by an amount that depends on gradients of the thermal pressure. In this model, the relevant TAE and RSAE frequencies are derived from several different references and are given by:

$$f_{TAE} = \frac{V_A}{4\pi q_{min} R} |(2 - (1 + 3\epsilon_g^2/4)^{1/2}|/(1 - \epsilon_g^2/4)^{1/2} \tag{1}$$

where

$$\epsilon_g = (\kappa^2 - 1)/(\kappa^2 + 1) \tag{2}$$

and

$$f_{RSAE-min}^2 = \left(f_{GAM}^2 + f_{\nabla}^2\right) \tag{3}$$

with the GAM frequency given by

$$f_{GAM}^2 = \frac{1}{4\pi^2}\left[\frac{2}{M_i R^2}\left(T_e + \frac{7}{4}T_i\right)\left(1 + \frac{1}{2q_{min}^2}\right)\right]\frac{2}{\kappa^2+1} \tag{4}$$

and the upshift in RSAE minimum frequency from the GAM frequency due to thermal plasma temperature gradients

$$f_\nabla^2 = \frac{-1}{2\pi^2 M_i R^2}\rho\frac{d}{d\rho}(T_e + T_i)\left(1 - \frac{1}{q_{min}^2}\right)\frac{2}{\kappa^2+1} \quad . \tag{5}$$

In the above, κ is the plasma elongation, V_A is the Alfvén speed, M_i is the ion mass, T_i ion temperature, T_e electron temperature, and R is major radius. The expressions for the TAE and GAM frequencies are modified from the standard cylindrical plasma expressions to include the effects of elongation and are adapted from Reference [15] using $\gamma = 1 + 3/4\frac{T_i}{T_e+T_i}$ for the ratio of specific heats. Without the elongation correction, the GAM frequency at high q_{min} reduces to that in Reference [9]. The gradient induced frequency upshift (f_∇) in $f_{RSAE-min}$ is from References [11, 14, 1] with the additional correction for elongation to be the same as that for f_{GAM} (see Equation 11 in Reference [15]). Note, we are ignoring contributions from the density gradient due to the fact that they are relatively small in the L-mode discharges presented here. The actual *ad-hoc* functional form for the frequency sweep of an individual RSAE is given in reference [3].

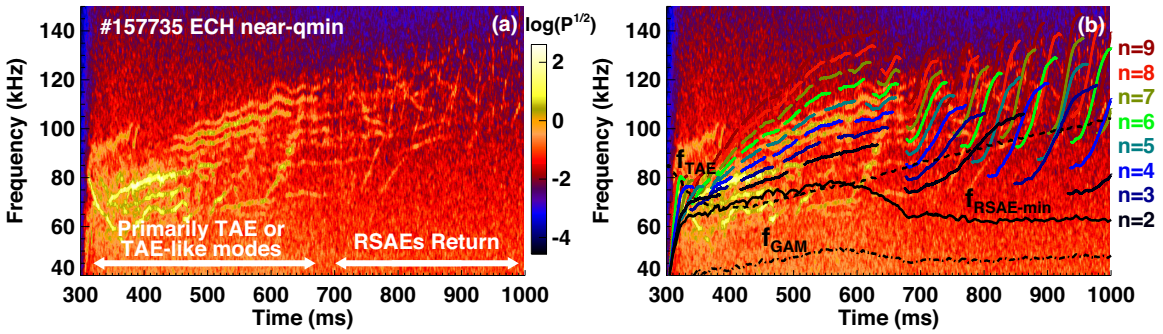

FIG. 2: (a) Combined ECE spectrogram for discharge 157735 with ECH heating near q_{min}. (b) Model for RSAE frequency evolution overlaid on same spectrogram from panel (a). Both ECH and NBI heating begin at $t = 300$ ms and extend over window shown.

Figure 2a shows a spectrogram for the "ECH near q_{min}" discharge 157735 presented in Figure 1c, except over a longer time window. In this figure, after approximately $t = 650$ ms, the activity shifts from primarily TAEs to a mix of RSAEs then essentially only RSAEs, despite deposition of ECH near mid-radius. The model RSAE spectra are shown overlaid on the spectrogram in Figure 2b along with f_{GAM}, $f_{RSAE-min}$ and f_{TAE}. Before $t \approx 600$ ms, $f_{RSAE-min}$ is near or above f_{TAE} and no frequency sweeping is predicted. After $t \approx 600$ ms, however, $f_{RSAE-min}$ drops precipitously and more typical frequency sweeping RSAEs are expected. This type of behavior is consistent with the beta suppression mechanism for RSAEs discussed by Fredrickson [9], with the exception that

the model here includes the additional gradient upshift of the RSAE minimum frequency. The rapid drop in $f_{RSAE-min}$ is due to a collapse of the core T_e profile which, as discussed in Reference [3], may be due to an increase in EP transport and reduced heating efficiency.

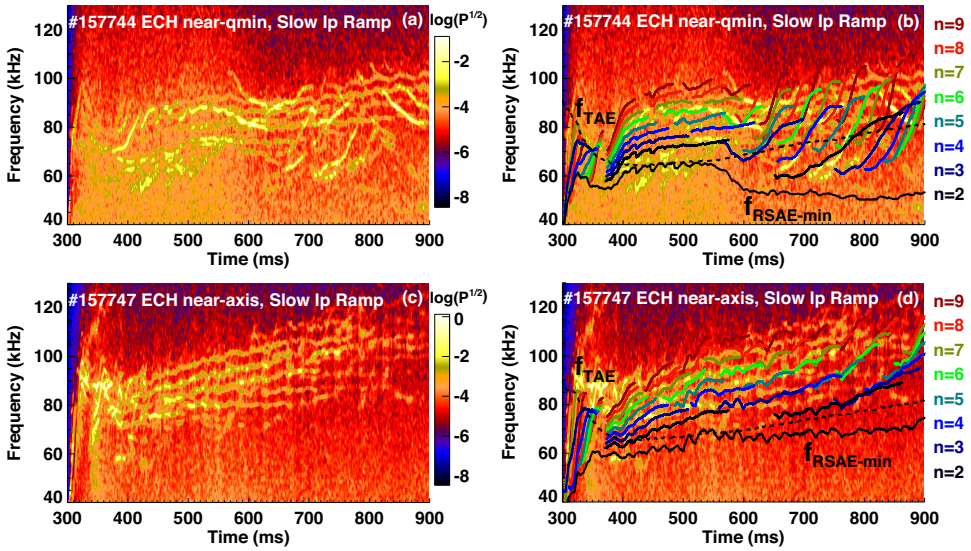

FIG. 3: Current ramp rate reduced from 0.8 MA/s to 0.44 MA/s. (a),(c) ECE spectrogram for discharge 157744 (157747) with ECH near q_{min}(Near axis). (b),(d) Model for RSAE freq. overlaid on spectra from panels (a),(c). ECH and NBI heating begin at $t = 300ms$.

Spectra from a set of discharges with somewhat different behavior are shown in Figure 3; in these discharges, the same ECH steering geometry and timing as Figures 1b-c was used but the current ramp rate was reduced from 0.8 MA/s to 0.44 MA/s. By reducing the current ramp rate, the impact of the ECH was essentially reversed relative to that in Figures 1b-c. In discharge 157747 with ECH near the magnetic axis (Figure 3c), the discharge is almost completely dominated by TAE-like modes, very little if any RSAE activity is apparent. For the slow current ramp ECH near q_{min} discharge (Figure 3a), there is a brief period ($t \approx 450 - 600$ ms) where frequency sweeping RSAEs are not clearly observed but it quickly returns to a case with a mix of RSAEs and TAEs. In both cases, motional Stark effect (MSE) data shows the safety factor profiles are reversed throughout the entire time windows shown. The model predictions for these discharges are given in Figure 3b and Figure 3d where excellent agreement with the measured behavior is shown. For the case with ECH near q_{min}, a brief period exists where $f_{RSAE-min}$ is near f_{TAE} and that period agrees well with the period of the discharge in which no frequency sweeping RSAEs are observed. Immediately following that period ($t \approx 600$ ms), RSAEs return, and this behavior is captured by the model. It is conjectured that a similar effect to that in Figure 2a must be occurring in this discharge that causes a rapid drop in T_e and consequently in $f_{RSAE-min}$. The predicted RSAE minimum frequency in discharge 157747, with ECH near the axis, on the other hand, remains elevated throughout the entire window shown and frequency sweeping RSAEs are not predicted or observed. The model again appears to capture the shift from frequency sweeping RSAEs to TAEs.

In the examples shown and essentially all other cases investigated (38+ discharges), the picture that RSAEs are observed only when $f_{RSAE-min} < f_{TAE}$ is consistent with the measured spectra. This statement is quantified in Figure 4, where the predicted $f_{RSAE-min}$ is plotted vs. f_{TAE} for several points during the current ramp portion of all discharges where AEs were observed. The points are color coded according to whether typical RSAEs were observed (RED) or not observed (BLACK). Overplotted is also where $f_{RSAE-min}$ $=f_{TAE}$. In Figure 4b, the data are also histogrammed vs. the ratio $f_{RSAE-min}/f_{TAE}$. A clear division exists between these two datasets; when $f_{RSAE-min} << f_{TAE}$ typical RSAEs are observed, while for $f_{RSAE-min} \lesssim f_{TAE}$ a mix of cases exists and for $f_{RSAE-min} > f_{TAE}$ typical frequency sweeping RSAEs are not observed.

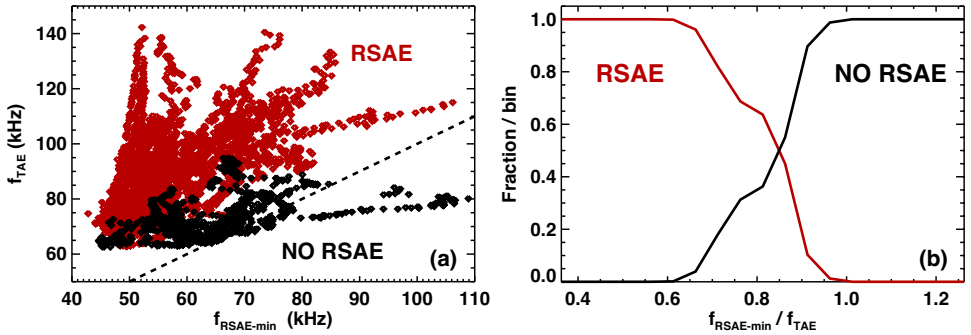

FIG. 4: Data from 38 discharges (t=0.3-1s). (a) Calculated $f_{RSAE-min}$ and f_{TAE} . RED/BLACK typical frequency sweeping RSAEs observed/not observed. Dashed line is f_{TAE} =$f_{RSAE-min}$. (b) Data from panel (a) histogrammed vs. the ratio f_{TAE} /$f_{RSAE-min}$

4 NOVA Simulations

NOVA simulations have been carried out for 157735, the "ECH near q_{min}" case (Figure 1c), near $q_{min} = 4$ and are presented in Figure 5. In these simulations, the minimum safety factor was scanned from $q_{min} = 4.02$ to $q_{min} = 3.79$ in order to resolve a full $n = 3$ RSAE frequency sweep ($n = 3$ is typically the strongest mode observed). In Figure 5, the right column represents $n = 3$ continua for a fixed q_{min} with a contour plot showing mode displacements vs. square root of normalized poloidal flux ($\psi^{1/2}$) and frequency. The left column of each figure displays the frequencies of all modes fitting the RSAE filtering criteria vs. q_{min}. Where the fundamental RSAE can be identified, its frequency evolution vs. q_{min} is followed by a red line. Here, the term fundamental RSAE refers to the highest frequency RSAE with no radial nodes in its eigenmode amplitude envelope [14, 2]. The goal of these calculations is to see if NOVA finds typical RSAEs for this scenario and to determine if the frequency sweeping RSAE is even an eigenmode of the experimental equilibrium, and to determine the impact of changing the pressure profile. Figure 5, shows calculations for $P = 0.15\times$, $0.33\times$ and $1.0\times$ the experimental pressure. The fundamental RSAE was not found for the experimental pressure case, except for possibly a very short q_{min} range (Figure 5c), however when the pressure is scaled down significantly (as would be expected with the removal of ECH), the fundamental frequency sweeping RSAE can be identified as is shown in Figures 5a-b.

At even 0.3× the experimental pressure, the fundamental RSAE is pushed inward and is found to interact with the continuum. In this equilibrium, for the experimental pressure, the typical RSAE is not an eigenmode of the system, instead, it is pushed very far into the TAE gap and strongly coupled to the TAEs found inside of q_{min}. The resulting mode has a mix of TAE and RSAE-like properties, something that is explained in Reference [3].

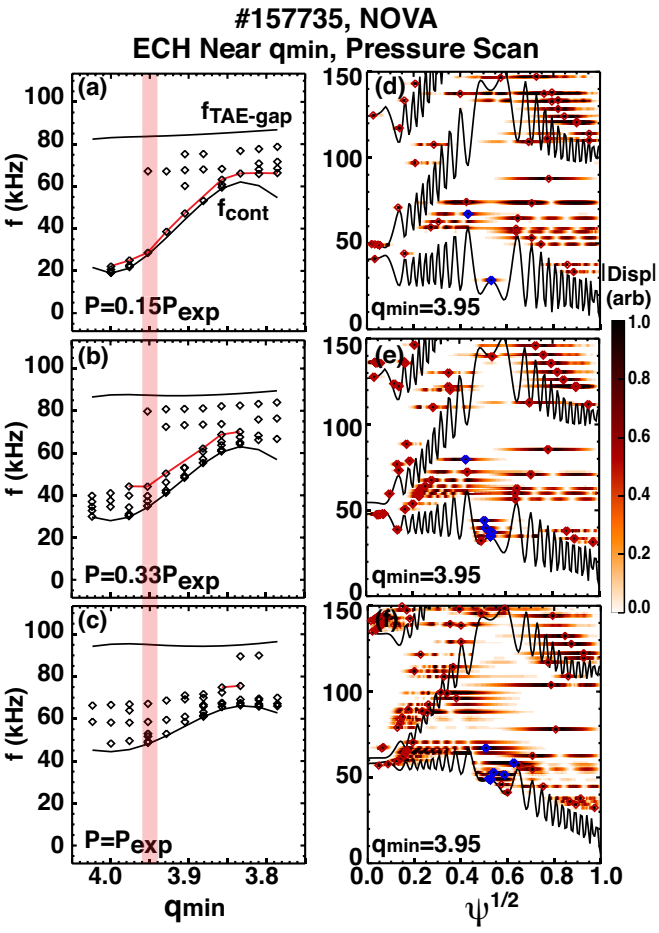

FIG. 5: $n = 3$ NOVA simulations discharge 157735 "ECH near q_{min}" with equil. pressure scaled to (a)&(d) $P = 0.15P_{exp}$, (b)&(e) $P = 0.33P_{exp}$, and (c)&(f) $P = P_{exp}$. (a)-(c) show "RSAE" frequencies with thin red line indicating fundamental RSAE. Solid black curves indicate continuum tip and center of TAE gap at q_{min}. Red bar indicates q_{min} that continua in panels (d)-(f) are shown for. Panels (d)-(f) have contours overlaid indicating eigenmode frequencies and displacement radial structure. Diamond markers are mode peak locations with blue indicating RSAE-like modes and red all other modes

5 Summary and Conclusions

Results have been presented from a recent DIII-D experiment and analysis focused on understanding the modification of beam driven RSAE activity by localized electron cyclotron heating. A database analysis of the current ramp phase in 38 discharges shows that the presence of frequency sweeping RSAEs is strongly dependent on the ratio of the RSAE minimum frequency (Equation 3) to TAE frequency (Equation 1), where the calculated RSAE minimum frequency includes an upshift from the GAM frequency (Equation 4) by an amount dependent on gradients in the local electron and ion temperatures (Equation 5). For $f_{RSAE-min}/f_{TAE} > 1$, no typical frequency sweeping RSAEs are observed. It is changes in this ratio through modification of electron temperature caused by ECH heating that is particularly effective at modifying the RSAE activity. Specifically, ECH can modify the local electron temperature at q_{min} as well as its gradient. Detailed ideal MHD calculations using the NOVA code show that for the ECH injection near q_{min} case, where no frequency sweeping RSAEs are observed experimentally, the typical frequency sweeping RSAE is no longer an eigenmode of the system. What remains is an eigenmode with poloidal harmonic content reminiscent of the standard RSAE, but absent of the typical

frequency sweeping behavior. The remaining eigenmode is also often strongly coupled to gap TAEs [3]. This new understanding, coupled with the fact that discharges with reduced RSAE activity also have improved fast ion confinement, offers worthwhile and intriguing possibilities for future AE control applications.

6 Acknowledgements

This work was carried out with support from the ITPA Energetic Particles Topical Group and contributes to the ITPA joint experiment EP-7 ("The Impact of Localized ECH on Alfvén Eigenmode Activity"). This material is based upon work supported in part by the U.S. Department of Energy, Office of Science, Office of Fusion Energy Sciences, using the DIII-D National Fusion Facility, a DOE Office of Science user facility, under Awards DE-FC02-04ER54698[1], SC-G903402[2], DE-AC05-00OR22725[4], DE-AC02-09CH11466[7]. The work of S.E. Sharapov was funded by RCUK Energy Programme [grant EP/I501045]. DIII-D data shown in this paper can be obtained in digital format by following the links at https://fusion.gat.com/global/D3D_DMP.

References

[1] M.A. Van Zeeland, *et al Plasma Phys. Control. Fusion* **50** 035009 (2008)

[2] M.A. Van Zeeland, *et al* Nucl. Fusion **49**, 065003 (2009).

[3] M.A. Van Zeeland, W.W. Heidbrink, S.E. Sharapov, *et al* Nucl. Fusion **56**, 112007 (2016).

[4] Nagasaki, et.al., 2012 Proc. 24th Int. Conf. on Fusion Energy, EX/P8-10

[5] K. Nagaoka, *et al Nucl. Fusion* **53** 072004 (2013)

[6] Y. Kusama, H. Kimura, T. Ozeki, , *et al* , Nucl. Fusion **38**, 1215 (1998).

[7] C. Z. Cheng, L. Chen, and M. S. Chance *Ann. Phys. (N.Y.* **161** 21 (1985)

[8] Chu M S, Greene J M, Lao, *et al Phs. Fluids B* **4** 3713 (1992)

[9] E. D. Fredrickson, *et al Phys. Plasmas* **14** 102510 (2007)

[10] C. Z. Cheng and M. S. Chance, J. Comput. Phys. **71**, 124 (1987).

[11] Breizman B N *Theory of Fusion Plasmas:Joint Varenna-Lausanne International Workshop* CP871 (2006)

[12] Sharapov S E *et al Phys. Plasmas* **9** 2027 (2002)

[13] D.A. Spong, *et al Phys. Plasmas* **19** 082511 (2012)

[14] Gorelenkov N N, *et al Plasma Phys Control. Fus.* **48** 1255 (2006)

[15] O.P. Fesenyuk, Ya. I. Kolesnichenko, and Yu. V. Yakovenko *Phys. Plasmas* **20** 122503 (2013)